IOP Conf. Series: Journal of Physics: Conf. Series **839** (2017) 012007 doi:10.1088/1742-6596/839/1/012007

Towards Modelling QFT in Real Metamaterials: Singular Potentials and Self-Adjoint Extensions

L M Nieto[1], **M Gadella**[1], **J Mateos Guilarte**[2], **J M Muñoz-Castañeda**[3], **and C Romaniega**[1,4]

[1] Departamento de Física Teórica, Atómica y Óptica and IMUVA, Universidad de Valladolid, Spain

[2] Departamento de Física Fundamental, Universidad de Salamanca, Spain

[3] Departamento de Física ETSIAE, Universidad de Politécnica de Madrid, Spain

[4] Departamento de Física Teórica II, Universidad de Complutense de Madrid, Spain

E-mail: luismiguel.nieto.calzada@uva.es, gadella@fta.uva.es, guilarte@usal.es, jose.munoz.castaneda@upm.es, csromaniega@gmail.com

Abstract. Solutions of the one-dimensional Schrödinger equation are found when point interactions of the type $a\delta(x-q)+b\delta'(x-q)$ are placed either in a couple of points or in a regular lattice. The results obtained in the present study are a first step toward a rigorous mathematical model of real metamaterials is Solid State Physics.

1. Introduction

One dimensional (1D) models with point interactions have received much attention in the recent literature (see Ref. [1] and references therein). They can model small and abrupt defects in materials allowing to perform analytic calculations such as the tunnel effect and the Casimir force. They are also interesting in the analysis of heterostructures in connection to an abrupt effective mass change. The general inquiry of point interactions of the free Hamiltonian $H_0=-\frac{\hbar^2}{2m}\frac{d^2}{dx^2}$ is mainly due to Kurasov [2] and it is based on the construction of self-adjoint extensions of symmetric operators with identical deficiency indices. Muñoz-Castañeda and coworkers [3] reformulated the theory of self-adjoint extensions of symmetric operators over bounded domains in terms of meaningful quantities from a Quantum Field Theory (QFT) point of view, allowing a rigorous study of the theory of quantum fields over bounded domains and the quantum boundary effects. In this context, it is well known that set of self-adjoint extensions of H_0 defined over the space $(-\infty,q)\cup(q,\infty)$ is given by the unitary group $U(2)$ and therefore is a 4-parameter family of operators. Some of some of these self-adjoint extensions are associated to the Hamiltonians H_0 plus point-supported potential $a\delta(x-q)+b\delta'(x-q)$, see [4]. This perturbation is of great interest in Quantum Mechanics from mathematical and physical points of view, and has been largely discussed in [4, 5]. Although it is totally clear which self-adjoint extension corresponds to the 1D-Dirac delta, there is no consensus on which one should be assigned to its derivative.

In the framework of QFT the spectra and eigenstates of non-relativistic Schrödinger operators provide one-particle states in scalar (1+1)-QFT systems. Point supported potentials can be used in scalar QFT on a line to model impurities and classical singular backgrounds that interact with quantum vacuum fluctuations. The most successful results in the frame of QFT are obtained in Casimir-type set-ups where the scattering data allow to compute the distance dependence finite part of the quantum vacuum energy for the quantum vacuum fluctuations that live between two plane parallel plates. In particular, configurations of two pure delta potentials added to the free Schrödinger Hamiltonian allowed to compute the quantum vacuum interaction energy between two parallel semitransparent Dirac δ-plates in terms of the scattering data of the pure double delta potential on the real line, see [5]. The same configuration of delta interactions is addressed as a perturbation of the Salpeter Hamiltonian. Additionally, generalized Dirichlet boundary conditions were discussed, showing that the use of δ-δ' potentials provides a much larger set of admissible boundary conditions, and the quantum vacuum energies between two plane parallel plates represented by a δ-δ' potential in arbitrary space-time dimension were computed [5].

Since the zero range potentials mimic the plates in a Casimir effect setup, it is interesting to consider a three-plate configuration (Casimir pistons) and investigate the Casimir forces acting of the plate in the middle that is supposed to be mobile in a piston configuration. In particular, it is meaningful to displace the central plate towards one of the other two placed in the boundary; thus, we find the main physical motivation to study the particular situation where two $\delta - \delta'$ interactions are superimposed. This is the first problem that will be addressed in Section 2, and the outcome is surprising: a non-abelian addition law emerges and it corresponds to the group law of the Borel subgroup of the $SL_2(\mathbb{R})$ group. The other focus of interest is the case where the δ'-couplings are exceptional, i.e., those couplings for which the transmission coefficients are zero and the plates become completely opaque: the left-right decoupling limit. It happens that the distinguished Dirichlet/Robin boundary conditions are implemented in this case by the $\delta - \delta'$-potentials but the superposition law just mentioned becomes singular [6].

An ideal model of electric conductivity in solids is provided by a δ-Dirac comb where δ-point interactions sit at the ions sites. This model can be enriched by adding a δ' potentials at every site of the lattice. This is the objective of Sec. 3, which is a work presently in progress [7].

2. One and two singular perturbations on a line

First of all, let us consider first the one-dimensional Schrödinger equation with singular potential

$$-\frac{\hbar^2}{2m}\frac{d^2}{dx^2}\,\psi(x) + a\delta(x-d)\psi(x) + b\delta'(x-d)\psi(x) = E\,\psi(x). \tag{1}$$

Introducing the dimensionless quantities $x = \frac{\hbar}{mc}y$, $d = \frac{\hbar}{mc}p$, $w_0 = \frac{2a}{\hbar c}$, $w_1 = \frac{mb}{\hbar^2}$, $\varepsilon = \frac{2E}{mc^2}$, and $\varphi(y) = \psi(x)$, the Hamiltonian is simply

$$-\frac{d^2}{dy^2}\,\varphi(y) + w_0\delta(y-p)\varphi(y) + 2w_1\delta'(y-p)\varphi(y) = \varepsilon\,\varphi(y). \tag{2}$$

The point potential we are interested in is usually defined via the theory of self-adjoint extensions of symmetric operators of equal deficiency indices, so that the total Hamiltonian in (2) is self-adjoint. The crucial point is to find the domain of wave functions $\varphi(y)$ that makes H_0 self-adjoint over the domain $\mathbb{R}/\{p\}$ and characterizes the potential $V(y)$. As these functions and their derivatives should have a discontinuity at $y = p$, we have to define the products of the form $\delta(y-p)\varphi(y)$ and $\delta'(y-p)\varphi(y)$. These can be done in several ways, and we choose the following:

$$\delta(y-p)\varphi(y) = \frac{\varphi(p^+) + \varphi(p^-)}{2}\,\delta(y-p)\,, \tag{3}$$

$$\delta'(y-p)\varphi(y) = \frac{\varphi(p^+) + \varphi(p^-)}{2}\,\delta'(y-p) - \frac{\varphi'(p^+) + \varphi'(p^-)}{2}\,\delta(y-p)\,. \tag{4}$$

To obtain a self-adjoint determination of $H = H_0 + V(y) = H_0 + w_0\delta(y-p) + 2w_1\delta'(y-p)$, we have to find a self-adjoint extension of H_0. To do it, we have to find a domain on which this extension acts, which is given by the Sobolev space $W_2^2(\mathbb{R}\setminus\{p\})$ of absolutely continuous functions $f(y)$ with absolutely continuous derivative $f'(y)$, both having arbitrary discontinuities at p, such that the Lebesgue integral given by

$$\int_{-\infty}^{\infty} \{|f(y)|^2 + |f''(y)|^2\}\, dy$$

converges, and such that at p satisfy the following matching conditions:

$$\begin{pmatrix} \varphi(p^+) \\ \varphi'(p^+) \end{pmatrix} = \begin{pmatrix} \dfrac{1+w_1}{1-w_1} & 0 \\ \dfrac{w_0}{1-w_1^2} & \dfrac{1-w_1}{1+w_1} \end{pmatrix} \begin{pmatrix} \varphi(p^-) \\ \varphi'(p^-) \end{pmatrix}. \tag{5}$$

These results could be extended to interactions of the type $\sum\big(a_i\delta(y-p_i) + 2b_i\delta'(y-p_i)\big)$, where the sum could be either finite or infinite.

2.1. Two singular perturbations on a line

We assume now that the total Hamiltonian is $H = H_0 + V + W$, with

$$H_0 = -\frac{d^2}{dy^2}, \qquad V = v_0\delta(y) + 2v_1\delta'(y), \qquad W = w_0\delta(y-p) + 2w_1\delta(y-p). \tag{6}$$

V is supported at the origin $y = 0$ and W is supported at $p > 0$. The potential $V + W$ is related to the Casimir effect. One of the motivations of this work is the study of the effect of the superposition of the two point potentials V and W at the same point (taking the limit as $p \to 0$). We shall see that we obtain a point potential of the type $u_0\delta(y) + 2u_1\delta'(y)$, where u_0 and u_1 are not the sums $v_0 + w_0$ and $v_1 + w_1$.

2.1.1. Matching conditions and scattering coefficients. In order to analyze $\varphi(y)$, the solution of (6), let us split the real line into the regions (1) $y < 0$, (2) $0 < y < p$, and (3) $p < y$, where

$$\varphi_i(y) = A_i\, e^{-iky} + B_i\, e^{iky}\,, \quad \varphi_i'(y) = -ik(A_i\, e^{-iky} - B_i\, e^{iky})\,, \quad i = 1,2,3\,, \quad k^2 = \varepsilon > 0.$$

Since the point potential V is defined by matching conditions like those in (5), we have

$$\begin{pmatrix} A_2 \\ B_2 \end{pmatrix} = K^{-1}\, M_v\, K \begin{pmatrix} A_1 \\ B_1 \end{pmatrix}, \quad M_v = \begin{pmatrix} \dfrac{1+v_1}{1-v_1} & 0 \\ \dfrac{v_0}{1-v_1^2} & \dfrac{1-v_1}{1+v_1} \end{pmatrix}, \quad K = \begin{pmatrix} 1 & 1 \\ -ik & ik \end{pmatrix}. \tag{7}$$

This expression gives the matching conditions at $y = 0$. At the point $y = p$ we get

$$\begin{pmatrix} A_3 \\ B_3 \end{pmatrix} = Q^{-1}\, K^{-1}\, M_w\, K\, Q\, K^{-1}\, M_v\, K \begin{pmatrix} A_1 \\ B_1 \end{pmatrix} = T_p \begin{pmatrix} A_1 \\ B_1 \end{pmatrix}, \tag{8}$$

where the definition of T_p is obvious, while Q and M_w are respectively:

$$Q = \begin{pmatrix} e^{-ipk} & 0 \\ 0 & e^{ipk} \end{pmatrix}, \qquad M_w = \begin{pmatrix} \dfrac{1+w_1}{1-w_1} & 0 \\ \dfrac{w_0}{1-w_1^2} & \dfrac{1-w_1}{1+w_1} \end{pmatrix}. \tag{9}$$

The T_p-matrix in (8) relates the asymptotic behavior of the two linearly independent Jost scattering solutions at $y \ll 0$ with their counterparts at $y \gg 0$. Remark that

$$\det T_p = T_p^{11} T_p^{22} - T_p^{12} T_p^{12} = 1 \ , \ T_p^{11} = \bar{T}_p^{22} \ , \ T_p^{12} = \bar{T}_p^{21} \quad \Rightarrow \quad T_p \in SL_2(\mathbb{C}).$$

From the T_p-matrix one obtains the 2×2 unitary scattering matrix S_p:

$$S_p = \frac{1}{T_p^{11}} \begin{pmatrix} 1 & -T_p^{12} \\ T_p^{21} & \det T_p \end{pmatrix} \ , \ S_p^\dagger = \frac{1}{\bar{T}_p^{11}} \begin{pmatrix} 1 & \bar{T}_p^{21} \\ -\bar{T}_p^{12} & \det T_p \end{pmatrix} \ , \ S_p^\dagger S_p = \begin{pmatrix} 1 & 0 \\ 0 & 1 \end{pmatrix} . \tag{10}$$

The transmission and reflection coefficients provide the usual form of writing the S_p matrix:

$$S_p = \begin{pmatrix} t(k) & r_R(k) \\ r_L(k) & t(k) \end{pmatrix}, \tag{11}$$

where $t(k)$ is the amplitude of the transmitted waves coming from the far left or from the far right. Time-reversal invariance implies $t_R(k;p) = t_L(k;p) = t(k;p)$. However, as the potential is not parity invariant, the reflection amplitudes are different for incoming waves either from the far right or the far left: $r_R(k;p) \neq r_L(k;p)$. We explicitly find:

$$\begin{aligned} r_L(k;p) &= -[e^{-2ipk}\left(2k\left(v_1^2+1\right)+iv_0\right)(4kw_1 - iw_0) + (4kv_1 - iv_0)\left(2k\left(w_1^2+1\right)-iw_0\right)]/\Delta(k), \\ r_R(k;p) &= [e^{2ipk}\left(2k\left(v_1^2+1\right)-iv_0\right)(4kw_1 + iw_0) + (4kv_1 + iv_0)\left(2k\left(w_1^2+1\right)+iw_0\right)]/\Delta(k), \\ t(k;p) &= 4k^2(1-v_1^2)(1-w_1^2)/\Delta(k), \end{aligned}$$

where $\Delta(k) = e^{2ikp}(v_0 + 4ikv_1)(w_0 - 4ikw_1) + (2kv_1^2 + 2k + iv_0)(2kw_1^2 + 2k + iw_0)$ is a function of k and the other parameters of the problem.

2.2. *Bound/antibound states and resonances*

Complex zeroes of $T_p^{11}(k) = \Delta(k)/[4k^2(1-v_1^2)(1-w_1^2)]$ (poles of the S_p-matrix) give rise to bound or antibound states if are located on the purely imaginary, respectively positive or negative half-axis. Complex zeroes coming in pairs having opposite real part and identical imaginary part correspond to resonances. Then the relevant physical information is encoded in the analysis of complex zeroes of $\Delta(k)$. If we make the changes

$$2kp = z, \quad \sigma = \frac{pv_0}{1+v_1^2}, \quad \tau = \frac{pw_0}{1+w_1^2}, \quad v = \frac{v_1}{1+v_1^2}, \quad w = \frac{w_1}{1+w_1^2}, \tag{12}$$

then, $\Delta(k) = 0$ is equivalent to

$$e^{iz} = -\left(\frac{z+i\sigma}{\sigma+2ivz}\right)\left(\frac{z+i\tau}{\tau-2iwz}\right), \quad z = z_r + iz_i, \ z_r, z_i \in \mathbb{R}. \tag{13}$$

Equation (13) is a generalization of the so-called *generalized Lambert equation*, from where we can obtain two real equations, corresponding to its real and imaginary parts

$$\left[4vwz_r^2 - (2vz_i - \sigma)(2wz_i + \tau)\right]\cos z_r - 2z_r(\tau v + 4vwz_i - \sigma w)\sin z_r = \left[(z_i+\sigma)(z_i+\tau) - z_r^2\right] e^{z_i}.$$

$$2z_r(\tau v + 4vwz_i - \sigma w)\cos z_r + \left[4vwz_r^2 - (2vz_i - \sigma)(2wz_i + \tau)\right]\sin z_r = -z_r(2z_i + \sigma + \tau)e^{z_i}.$$

A simpler compatibility condition is this Lambert equation in two real variables

$$e^{2z_i} = \frac{\left(4v^2z_r^2 + \left(2vz_i - \sigma\right)^2\right)\left(4w^2z_r^2 + (2wz_i + \tau)^2\right)}{\left(z_r^2 + (z_i+\sigma)^2\right)\left(z_r^2 + (z_i+\tau)^2\right)}. \tag{14}$$

We can easily check that a simple solution of the system is $z_r = 0$, $z_i = 0$, but this corresponds to $k = 0$, which is a pole of $T_p^{11}(k)$. The typical behavior of the solutions of these equations is shown in Fig. 1, where the blue curves are the real part, the yellow ones the imaginary part and the green curve is the compatibility condition (14).

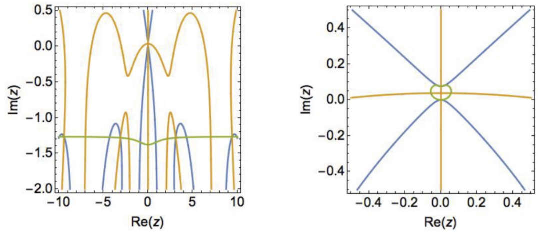

Figure 1.

2.3. The addition law at the $p = 0$ limit

We can summarize what happens in the limit $p \to 0$ as follows: the T_p matrix for two-pairs of $\delta - \delta'$ interactions displaced from each other a distance p becomes:

$$\begin{pmatrix} A_3 \\ B_3 \end{pmatrix} = K^{-1} M_w \cdot M_v K \begin{pmatrix} A_1 \\ B_1 \end{pmatrix} = K^{-1} M_u K \begin{pmatrix} A_1 \\ B_1 \end{pmatrix}. \tag{15}$$

Then, the superposition of these two $\delta - \delta'$ is equivalent to a single $\delta - \delta'$ where the matching conditions are characterized by the Kurasov matrix

$$M_u = \begin{pmatrix} \dfrac{1+u_1}{1-u_1} & 0 \\ \dfrac{u_0}{1-u_1^2} & \dfrac{1-u_1}{1+u_1} \end{pmatrix}, \qquad u_1 = \frac{v_1 + w_1}{1 + v_1 w_1}, \quad u_0 = \frac{v_0(1-w_1)^2 + w_0(1+v_1)^2}{(1+v_1 w_1)^2}. \tag{16}$$

This addition law is quite interesting. It can be proved [6] that the Kurasov matrices is the Borel subgroup of $SL_2(\mathbb{R})$, with the product law $M_v \cdot M_w = M_u$ given by (16). It can be also shown that the $p \to 0$ limit of the scattering coefficients of two a priori separated pairs of $\delta - \delta'$ interactions is

$$\lim_{p \to 0} S_p(M_v, M_w) = S(M_v \cdot M_w) = S(M_u) \tag{17}$$

Hence, the scattering matrices produced by two superimposed pairs of $\delta - \delta'$ interactions give rise to a representation of the non-abelian composition law of Kurasov matrices. In other words, the non-abelian addition law (16) also works for the scattering coefficients.

2.4. The left-right decoupling values of the δ' couplings

It is interesting to stress that there are singularities of the Kurasov matrix M_v, M_w in (7) and (9) at the critical points $v_1 = \pm 1$ and $w_1 = \pm 1$. One may expect that these critical cases, where the transmission coefficients are zero, do not contribute to the group structure that we have previously explained. The completely opaque potentials have one of the following forms:

$$V = v_0 \delta(y) \pm 2\delta'(y) \quad \text{and/or} \quad W = w_0 \delta(y-p) \pm 2\delta'(y-p). \tag{18}$$

In order to define these potentials, we cannot use the same matching conditions as before. Instead, following the work of Kurasov, we shall impose:

(i) For $v_1 = 1$: $\varphi(0^-) = 0$, $\varphi'(0^+) = v_0\, \varphi(0^+)/4$.
(ii) For $w_1 = 1$: $\varphi(p^-) = 0$, $\varphi'(p^+) = w_0\, \varphi(p^+)/4$.
(iii) For $v_1 = -1$: $\varphi(0^+) = 0$, $\varphi'(0^-) = -v_0\, \varphi(0^-)/4$.
(iv) For $w_1 = -1$: $\varphi(p^+) = 0$, $\varphi'(p^-) = -w_0\, \varphi(p^-)/4$.

Thus, we set Dirichlet boundary conditions on one side of the two points $y = 0$ and $y = p$, whereas Robin boundary conditions are chosen on the other. There are eight possible configurations involving at least one decoupling configuration of the couplings: either the two $\delta - \delta'$ interactions build opaque walls both at $y = 0$ and $y = p$, or there is no transmission only at one point. We discuss first the four cases when the two δ' couplings take the decoupling limit.

2.4.1. Two δ' couplings in the decoupling limit. There are four cases in which we have decoupling situations both at $y = 0$ and $y = p$. Let us consider them separately.

Case 1: $v_1 = 1, w_1 = 1$. The boundary conditions are given by $\varphi(0^-) = 0$, $\varphi'(0^+) = v_0\,\varphi(0^+)/4$, $\varphi(p^-) = 0$, $\varphi'(p^+) = w_0\,\varphi(p^+)/4$. For $y = 0^+$, the condition is written as:

$$-ik(A_2 - B_2) = \frac{v_0}{4}(A_2 + B_2) \Longrightarrow \frac{A_2}{B_2} = -\frac{v_0 - 4ik}{v_0 + 4ik} = -\exp\left(-2i \arctan\frac{4k}{v_0}\right). \tag{19}$$

For $y = p^-$, we obtain $A_2\, e^{-ikp} + B_2\, e^{ikp} = 0$. Then, we have a transcendental equation, which can be written either in the form of a generalized Lambert equation $e^{2ikp} = (v_0 - 4ik)/(v_0 + 4ik)$, or $\tan(kp) = -4k/v_0$. This equation has a countably infinite number of solutions, k_n, that give the energy levels corresponding to this case. In the limit $p = 0$, we have only one solution, $k = 0$. Outside the interval $[0, p]$, we have the equations

$$\varphi(0^-) = 0 \Longrightarrow A_1 + B_1 = 0 \qquad \varphi'(p^+) = \frac{w_0}{4}\varphi(p^+) \Longrightarrow \frac{A_3}{B_3} = -e^{2ikp}\frac{w_0 - 4ik}{w_0 + 4ik}. \tag{20}$$

These are relations between coefficients, which do not provide of any further information, so that we shall not refer for similar situations which will appear for all other cases.

Case 2: $v_1 = 1$, $w_1 = -1$. The boundary conditions are $\varphi(0^-) = 0$, $\varphi'(0^+) = v_0\,\varphi(0^+)/4$, $\varphi(p^+) = 0$, $\varphi'(p^-) = -w_0\,\varphi(p^-)/4$. The condition at $y = 0$ has already been studied. From the new boundary condition at $y = p$:

$$-kp = \arctan\frac{4k}{w_0} + \arctan\frac{4k}{v_0} \quad \Longrightarrow \quad \tan(kp) = -\frac{4k(w_0 + v_0)}{w_0 v_0 - 16k^2}. \tag{21}$$

This new transcendental equation gives another set of energy eigenvalues, seen in the left hand side of next Figure. In the limit $p \to 0$, we have only one solution: $k = 0$.

Case 3: $v_1 = -1$, $w_1 = 1$. The boundary conditions are such that $A_2 + B_2 = 0$ and $\varphi(p^-) = 0$, which is $A_2/B_2 = -e^{2ikp}$, so that

$$\frac{A_2}{B_2} = -1 = -e^{-2ikp} \Longrightarrow k = \frac{\pi n}{p}. \tag{22}$$

Again, in the limit $p = 0$, the only solution is $k = 0$.

Case 4: $v_1 = -1$, $w_1 = -1$. This correspond to $\varphi(0^+) = 0$, $\varphi'(0^-) = -v_0\,\varphi(0^-)/4$, $\varphi(p^+) = 0$, $\varphi'(p^-) = -w_0\,\varphi(p^-)/4$. Then, the transcendental equation giving the energy levels is given by

$$e^{2ikp} = \frac{w_0 - 4ik}{w_0 + 4ik} \quad \Longleftrightarrow \quad \tan(kp) = -(4k)/(w_0). \tag{23}$$

This transcendental equation also has a countably infinite number of solutions, k_n, that give the energy levels corresponding to this situation, seen in the right hand side of Fig. 2. Once more, in the limit $p \to 0$, only the solution $k = 0$ remains.

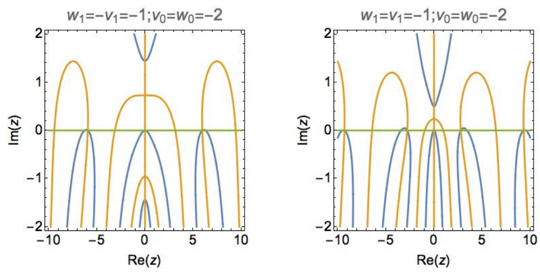

Figure 2.

2.4.2. Only one δ' coupling in the decoupling limit. Let us consider the following four cases:

Case 1: $v_1 = 1, w_1 \neq \pm 1$. Skipping the technical details, the system behaves as if there is an impenetrable barrier at $y = 0$. The coefficients A_3, B_3 are obtained from A_2, B_2:

$$\begin{pmatrix} A_3 \\ B_3 \end{pmatrix} = \begin{pmatrix} \dfrac{2k(1+w_1^2)+iw_0}{2k(1-w_1^2)} & e^{2ikp}\,\dfrac{4kw_1+iw_0}{2k(1-w_1^2)} \\ e^{-2ikp}\,\dfrac{4kw_1-iw_0}{2k(1-w_1^2)} & \dfrac{2k(1+w_1^2)-iw_0}{2k(1-w_1^2)} \end{pmatrix} \begin{pmatrix} A_2 \\ B_2 \end{pmatrix}. \tag{24}$$

All the relevant information about bound states, anti-bound states and resonances is obtained imposing the *purely outgoing boundary condition*, which in our case is $A_3 = 0$. Then, we get

$$e^{2ikp} = \frac{v_0 - 4ik}{v_0 + 4ik}\,\frac{2k(1+w_1^2)+iw_0}{4kw_1+iw_0}. \tag{25}$$

This equation is the equivalent of $\Delta(k) = 0$, which provides the relevant information in the non-decoupling case. Indeed, (25) is obtained making $v_1 = 1$ in $\Delta(k) = 0$. The analysis in this case is similar to the one carried out previously. We are very interested in the limit $p \to 0$. Then, from (25) we get $(v_0 + 4ik)(4kw_1 + iw_0) = (v_0 - 4ik)(2k(1 + w_1^2) + iw_0)$. The complex solutions of this equation are $k_0 = 0$, $k_1 = -i(4w_0 + v_0(1 - w_1)^2)/(4(1 + w_1)^2)$. The solution $k = 0$ is not relevant, but the other produces interesting results:

- If $4w_0 + v_0(1 - w_1)^2 < 0$, k_1 is on the positive imaginary axis and it is a bound state.
- If $4w_0 + v_0(1 - w_1)^2 > 0$, k_1 is on the negative imaginary axis and it is an anti-bound state.

The curves solving the equations $\mathrm{Re}(\Delta) = 0$ (blue) and $\mathrm{Im}(\Delta) = 0$ (yellow) are represented on the left hand side of the next Figure (the green line is the real exis).

Case 2: $v_1 = -1$, $w_1 \neq \pm 1$. The system behaves also as if there were an impenetrable barrier at $y = 0$. Now, the *purely outgoing boundary condition* $A_3 = 0$ implies that $e^{2ikp} = (2k(1 + w_1^2) + iw_0)/(4kw_1 + iw_0)$. See the right hand side of Fig. 3. In the limit $p \to 0$ we get the unique solution $k = 0$.

Case 3: $v_1 \neq \pm 1$, $w_1 = 1$. It is similar to the previous one.

Case 4: $v_1 \neq \pm 1$, $w_1 = -1$. This is similar to the first case studied before. Imposing the *purely outgoing boundary condition* $B_1 = 0$, we get

$$e^{2ikp} = -\frac{w_0 - 4ik}{w_0 + 4ik}\,\frac{2k(1+v_1^2)+iv_0}{4kv_1-iv_0}. \tag{26}$$

In the limit $p \to 0$, we have the complex solutions $k_0 = 0$, $k_1 = -i(4v_0 + w_0(1+v_1)^2)/(4(1-v_1)^2)$. The solution $k = 0$ is not relevant, but the other one, k_1, corresponds either to a bound state if $4v_0 + w_0(1 + v_1)^2 < 0$, or to an anti-bound state if $4v_0 + w_0(1 + v_1)^2 > 0$.

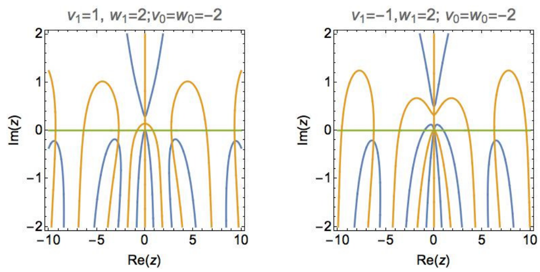

Figure 3.

3. A hybrid $\delta-\delta'$ Dirac comb

A very well known example of exactly solvable periodic potential used in Solid State Physics is the Kronig-Penney model, which describes electron motion in a period array of rectangular barriers. The Dirac-Kronig-Penney model can be considered as a special case of the Kronig-Penney model obtained by taking the appropriate limit in such a way that the rectangular barriers become Dirac delta distributions. Hence, very naturally comes the idea of considering a modified Dirac comb adding a δ' in every singular point. The dimensionless Schrödinger equation for such an hybrid Dirac comb becomes:

$$-\frac{d^2\psi(y)}{dy^2}+\left(\sum_{n\in\mathbb{Z}}\left[w_0\delta(y-na)+2w_1\delta'(y-na)\right]\right)\psi(y)=\varepsilon\,\psi(y). \tag{27}$$

To solve it, first, we will solve the equation in $(-a,0)$ (region I) and $(0,a)$ (region II):

$$\psi_I(y)=A_I\,e^{iky}+B_I\,e^{-iky},\qquad \psi_{II}(y)=A_{II}\,e^{iky}+B_{II}\,e^{-iky}\;,\quad \varepsilon=k^2. \tag{28}$$

Hence, $\psi_I'(y)=ikA_I\,e^{iky}-ikB_I\,e^{-iky}$, $\psi_{II}'(y)=ikA_{II}\,e^{iky}-ikB_{II}\,e^{-iky}$. In compact matrix form, these solutions can be written as follows ($J=I,II$):

$$\begin{pmatrix}\psi_J(y)\\ \psi_J'(y)\end{pmatrix}=K\,Q_y\begin{pmatrix}A_J\\ B_J\end{pmatrix},\qquad K=\begin{pmatrix}1&1\\ ik&-ik\end{pmatrix},\quad Q_y=\begin{pmatrix}e^{iky}&0\\ 0&e^{-iky}\end{pmatrix}. \tag{29}$$

Now, we impose Kurasov's matching conditions at $y=0$, as in the previous Section:

$$\begin{pmatrix}A_{II}\\ B_{II}\end{pmatrix}=K^{-1}T_wK\begin{pmatrix}A_I\\ B_I\end{pmatrix}. \tag{30}$$

Finally, as the potential is periodic, Floquet-Bloch theory establishes that for a periodic potential of period a, the wave functions are quasi-periodic, a plane wave times a periodic function:

$$\psi(y)=e^{iqy}\phi(y)\,,\quad q\in\mathbb{R}\,,\;\; q\simeq q+\frac{2\pi}{a}n\,,\;\; n\in\mathbb{Z}\;,\qquad \phi(y+a)=\phi(y)\;,$$

which implies that $\psi(y+a)=e^{iqa}\psi(y)$, henceforth $\psi'(y+a)=e^{iqa}\psi'(y)$. The Floquet index q is conventionally referred to as *quasi-momentum*. Thus, we write for $y\in(-a,0)$,

$$\begin{pmatrix}\psi_{II}(y+a)\\ \psi_{II}'(y+a)\end{pmatrix}=e^{iqa}\begin{pmatrix}\psi_I(y)\\ \psi_I'(y)\end{pmatrix}. \tag{31}$$

Using the explicit form of the solutions in that equation we get

$$KQ_yQ_a\begin{pmatrix}A_{II}\\ B_{II}\end{pmatrix}=e^{iqa}KQ_y\begin{pmatrix}A_I\\ B_I\end{pmatrix}. \tag{32}$$

IOP Conf. Series: Journal of Physics: Conf. Series **839** (2017) 012007 doi:10.1088/1742-6596/839/1/012007

In order to find non-trivial solution, we must have $\det\left[e^{iqa}\,\mathbb{I}-Q_aK^{-1}T_wK\right]=0$. After some algebra, we obtain the following *dispersion relation* guaranteeing that the determinant is null:

$$\cos qa = f(w_1)\left[\cos ka+\frac{a}{2}w_0\;g(w_1)\,\frac{\sin ka}{ka}\right],\qquad f(w_1)=\frac{1+w_1^2}{1-w_1^2},\quad g(w_1)=\frac{1}{1+w_1^2}. \tag{33}$$

If the δ' interactions are switched off, $w_1=0$, the band spectral equation for the standard Dirac comb reappears. On the other hand, if we define the 2×2-matrix $\Omega^{(1)}=\mathbb{M}_a\mathbb{K}^{-1}\mathbb{T}_w\mathbb{K}$, the band spectrum condition or dispersion relation can re-written as $\cos(qa)=\mathrm{tr}(\Omega^{(1)})/2$. Since $\cos(qa)\in(-1,1)$ only those momenta/energies that satisfy $\left|\mathrm{tr}(\Omega^{(1)})\right|\leq 2$ comply with the spectral condition and therefore characterize the *allowed band spectrum* of the ideal 1D crystal described by the $\delta-\delta'$ comb.

3.1. Analysis of the structure of the band spectrum

The analysis of the band structure of the energy spectrum of a periodic but not even potential with period a demands the solution of the transcendent equation:

$$\begin{aligned}\cos qa &= \frac{\left[t^2(k)-r_R(k)r_L(k)+1\right]\cos ka+i\left[t^2(k)-r_R(k)r_L(k)-1\right]\sin ka}{2t(k)} \\ &= \frac{\cos\left[ka+\delta(k)\right]}{|t(k)|},\end{aligned} \tag{34}$$

which depends only on the scattering data for a single point-potential. In the case of a single $\delta-\delta'$ interaction in the $y\in[0,a)$ interval these magnitudes are:

$$t(k)=\frac{(1-w_1^2)k}{(1+w_1^2)k+iw_0/2},\qquad |t(k)|=\frac{2|k||1-w_1^2|}{\sqrt{4k^2(1+w_1^2)^2+w_0^2}},$$

$$r_R(k)=-\frac{2kw_1+iw_0/2}{(1+w_1^2)k+iw_0/2},\qquad r_L(k)=\frac{2kw_1-iw_0/2}{(1+w_1^2)k+iw_0/2},$$

$$\delta(k)=\frac{1}{2i}\log\left(t^2(k)-r_R(k)r_L(k)\right)=\frac{1}{2i}\log\frac{2ik(1+w_1^2)+w_0}{2ik(1+w_1^2)-w_0}+\theta(w_1^2-1)\pi,$$

where $\theta(x)$ is the Heaviside step function. Notice that the reflection amplitudes for incoming particles from either the left or the right are different since the δ' coupling breaks parity invariance. Time reversal invariance, however, is preserved and the transition amplitude is the same whatever the incoming direction of the particle is.

It follows that a given value of k belongs to an allowed band if

$$\frac{1}{|t(k)|}\cos\left(ka+\delta(k)\right)\leq 1.$$

The right hand side of (34) is an oscillating function of k that tends asymptotically to a periodic function of amplitude $1/|t(k\to\pm\infty)|\geq 1$. Thus, there are pairs of points k_j and k_{j+1} where

$$\cos\left(k_ja+\delta(k_j)\right)/|t(k_j)|=\pm 1\quad\text{and}\quad\cos\left(k_{j+1}a+\delta(k_{j+1})\right)/|t(k_{j+1})|=\mp 1,$$

which are the edges of allowed bands: in the intervals $[k_j,k_{j+1}]$ the spectral function varies between ± 1 and ∓ 1, and there are intersections with the k-independent functions $g=\cos qa\in[-1,1]$, giving solutions of the spectral equation. In the interval (k_{j+1},k_{j+2}), where k_{j+2} is the next point for which $\cos\left(k_{j+2}a + \delta(k_{j+2})\right)/|t(k_{j+2})| = \mp 1$, the modulus of the spectral function is greater than one and there are no solutions: we find a forbidden band or gap.

The distribution of allowed and forbidden bands in the hybrid Dirac comb depends thus of the w_0 and w_1 couplings through the dependence in these parameters of the scattering data. There are several points and/or lines in the parameter space (w_0, w_1) that lead to critical behavior:

(i) The origin: $(w_0 = 0, w_1 = 0)$. In this case $|t(k)| = 1$, $\forall k$, and there is only one allowed band: the whole real line. Trivially, we end with the continuous spectrum of the free particle. All the forbidden bands disappear.

(ii) The infinite lines: $(w_0 = \pm\infty, w_1)$. When the point δ-interactions are either infinitely repulsive walls or attractive wells the transition amplitudes are null, $|t(k)|_{w_0=\pm\infty} = 0$, for all k. There are only solutions to the secular equation (or dispersion relation) (34) if $\cos\left(ka + \delta(k)\right)|_{w_0=\pm\infty}$ is also zero. Because $\delta(k)|_{w_0=\pm\infty} = i\pi$ this happens only if

$$k_n = \frac{\pi}{a}n, \quad \text{where} \quad n \in \mathbb{Z}.$$

The spectrum is purely discrete and all the allowed bands collapse to a point. The reflection amplitudes are constant, $r(k, \pm\infty, w_1) = -1$, and the eigenfunctions are standing waves with n nodes between two adjacent impenetrable walls/wells. Notice that, given a fixed n, there is an infinite number of eigenfunctions with energy proportional to $\varepsilon_n = k_n^2$. All the other possibilities interpolate between these two extreme cases. There are however other exceptional cases.

(iii) The singular lines: $(w_0, w_1 = \pm 1)$. Over thes two lines in the space of couplings the $\delta - \delta'$ potentials are also opaque: $t[k, w_0, \pm 1] = 0$. There are solutions of the equation (34) if and only if:

$$k_n a + \delta(k_n) = k_n a + \frac{1}{2}\mathrm{Arg}\left[\frac{w_0 i - 4k_n}{w_0 i + 4k_n}\right] + \frac{\pi}{2} = (n + \frac{1}{2})\pi \ \ , \ n \in \mathbb{Z} \ .$$

All the allowed bands collapse to points and the spectrum is discrete. The dependence on n of the physical momenta k_n is not linear like in the previous case because the reflection amplitudes are not trivial and phase shifts vary with k, specially at low momenta:

$$r_R[k, w_0, -1] = r_L[k, w_0, 1] = \frac{4k - iw_0}{4k + iw_0} \quad , \quad r_R[k, w_0, 1] = r_L[k, w_0, -1] = -1 \,.$$

The standing wave eigenfunctions incorporate in this case phase shifts after rebounding at the walls.

(iv) The ordinate axis: $(w_0 = 0, w_1)$. In this limit where only the δ'-coupling w_1 is non null we find a pathological behaviour. All the scattering amplitudes are independent of the energy:

$$t[k, 0, w_1] = \frac{1 - w_1^2}{1 + w_2^2}\,, \qquad r_R[k, 0, w_1] = -\frac{2w_1}{1 + w_1^2}\,, \qquad r_L[k, 0, w_1] = \frac{2w_1.}{1 + w_1^2}\,.$$

Moreover, the phase shifts in the even and odd channels are also k-independent

$$\delta_+(k, 0, w_1) = \frac{1}{2}\mathrm{Arg}\left[\frac{2|w_1|}{1 - w_1^2}\right], \qquad \delta_-(k, 0, w_1) = -\frac{1}{2}\mathrm{Arg}\left[\frac{2|w_1|}{1 - w_1^2}\right],$$

but the total phase shift is $\delta(k, 0, w_1) = \delta_+(k, 0, w_1) + \delta_-(k, 0, w_1) = 0$. Thus, the secular equation simplify to

$$\cos qa = \frac{1 + w_1^2}{|1 - w_1^2|}\cos ka. \tag{35}$$

3.2. More details on the distribution of allowed and forbidden bands in the hybrid Dirac comb

Another interesting line in the plane of couplings is the axis $w_1 = 0$. There is no δ' interaction which means that $f(0) = g(0) = 1$ and the spectral equation reduces to the well known secular equation for the Dirac comb potential:

$$\cos qa = \cos ka + aw_0(2ka)^{-1}w_0 \sin(ka)\,, \tag{36}$$

which identifies the band edge points as the discrete solutions of the transcendent equations:

$$\sqrt{\frac{4k_j^2 + w_0^2}{4k_j^2}} \cos\left[k_j a + \frac{1}{2}\mathrm{Arg}(4k_j^2 - w_0^2 + 4ik_j w_0)\right] = \pm 1\,. \tag{37}$$

Implicitly we have focused until now on solutions to the secular equations for *real momenta*, $k \in \mathbb{R}$, corresponding to propagating (conducting) band states.

Another important band state solutions respond to purely imaginary momenta, $k = i\kappa$, $\kappa \in \mathbb{R}$, which give rise to non-propagating states filling the so called valence bands. For the Dirac comb arrangement with attractive couplings the secular equation for purely imaginary momenta is well known:

$$\cos qa = v(\kappa, a, |w_0|)\,, \qquad v(\kappa, a, |w_0|) = \cosh \kappa a - \frac{a}{2}|w_0|\frac{\sinh \kappa a}{\kappa a}\,, \tag{38}$$

One checks easily that $v(0, a, |w_0|) = 1 - \frac{a}{2}|w_0|$ and that $\frac{\partial v}{\partial \kappa}(\kappa, a, |w_0|)\Big|_{\kappa=0} = 0$. Thus, $\kappa = 0$ is a critical point of the even function $v(\kappa, a, |w_0|)$. In the range $0 < |w_0| < \frac{4}{a}$ the spectral function v intersects with the straight line $v_0 = 1$ at two points $\pm\kappa_1$. Moreover, in this range the function v is always less than 1 but greater than -1 in the interval $\kappa \in [-\kappa_1, \kappa_1]$. Thus, there is one valence band with upper and lower edge points respectively of zero and $-\kappa_1^2$ energy.

Note that $\kappa = 0$ is a minimum of v, whereas $1 > v > -1$. Observe also that $\lim_{\kappa\to\pm\infty}(\kappa, a, |w_0|) = +\infty$. If $\frac{4}{a} < |w_0| < \frac{6}{a}$ the spectral function v intersect also with the straight line $v_0 = -1$ at the points $\pm\kappa_2$. $\kappa = 0$ is still the minimum of v but it does not belong to the valence band and the upper edge energy $-\kappa_2^2$ is lower than zero. For $\frac{6}{a} < |w_0|$ the band structure of negative energy states is similar but a little more subtle because $\kappa = 0$ becomes a local maximum of v prompting also the appearance of two minima of v at $\kappa = \pm\kappa_0$. For attractive coupling stronger than this the valence band width becomes more and more thin.

3.3. Differences between the band structures of the hybrid and standard Dirac combs

The strategy to analyze the differences between the band structures will be to fix a value of w_0, the strength of the δ-coupling, and to study, mainly graphically, how the solutions of the secular equation vary with w_1. In particular, variations in the width of the forbidden and allowed bands as function of the δ'-coupling w_1 will inform us about the modulation of the band distribution of the hybrid Dirac comb.

To start with we recall again that, since $|\cos(qa)| \leq 1$, the allowed bands are characterized by the inequality:

$$\left| f(w_1)\left[\cos(a\sqrt{\varepsilon}) + \frac{a}{2}w_0\, g(w_1)\,\frac{\sin(a\sqrt{\varepsilon})}{a\sqrt{\varepsilon}}\right]\right| \leq 1\,. \tag{39}$$

Here, we have written the dispersion relation in terms of $\varepsilon = k^2$ instead of using k as independent variable. This election of independent variable allows us to encode as a function of a single real variable the spectral function determining both the valence and conduction bands, without the need of going to the complex k-plane. The use of k as the independent variable in the spectral

IOP Conf. Series: Journal of Physics: Conf. Series **839** (2017) 012007 doi:10.1088/1742-6596/839/1/012007

function that characterize the bands requires that the conducting bands lie in the real k-axis while the valence bands are found in the pure imaginary $k = i\kappa$-axis. Thus, we shall plot both the valence bands, if they exists, the values of the energy where the inequality (39) is satisfied with $\varepsilon < 0$, and the conduction bands, energy intervals compatible with (39) for $\varepsilon > 0$, in a single $2D$ graphic.

This work is presently in progress [7] and we present here just some plots. For example, in Fig. 4 we show a plot of the allowed (yellow) and forbidden (blue) energy bands inferred from the spectral condition for $w_0 = -0.5$ and $a = 1$. In the graphic on the left it is seen how the width of several energy bands complying with the inequality (39) varies with w_1. Forbidden energy bands missing this inequality are also plotted in blue. The graphic on the right shows only the lowest allowed and forbidden energy bands for identical choice of w_0. This zoom of the graphic allows to recognize the merging of the valence with the lower conduction band at values of w_1 slightly greater than 0. Note also that the secular equation is invariant under the exchange $w_1 \leftrightarrow -w_1$. Thus, there are mirror images of the Figures shown here on the negative w_1-axis.

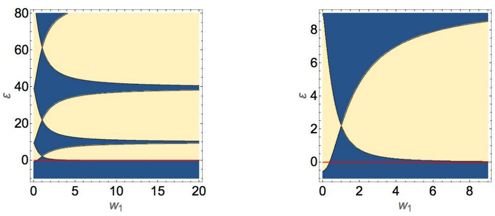

Figure 4.

Acknowledgments

LMN thanks the organizers of Quantum Fest 2016 (IPN-México City) for their kind invitation to give three talks. Partial financial support of Spanish MINECO (MTM2014-57129-C2-1-P) and Junta de Castilla y León (VA057U16) is acknowledged.

References

[1] Albeverio S, Gesztesy F, Hoegh-Krohn R and Holden H 2005 *Solvable models in quantum mechanics* (Providence, RI: AMS Chelsea Publishing)

[2] Kurasov P 1996 *J. Math. Anal. Appl.* **201** 297; S Albeverio, P Kurasov 2000 *Singular perturbations of differential operators. Solvable Schrödinger type operators*, London Mathematical Society Lecture Notes 271, (Cambridge: Cambridge UP).

[3] Asorey M, García-Alvarez D and Muñoz-Castañeda J M 2006 *J. Phys A: Math. Theor* **39** 6127-6136; Asorey M and Muñoz-Castañeda J M 2013 *Nucl. Phys. B* **874** 852876; Muñoz-Castañeda J M, Kirsten K and Bordag M 2015 *Lett. Math. Phys.* **105** 523549.

[4] Muñoz-Castañeda J M, Mateos Guilarte J and Moreno Mosquera A 2013 *Phys. Rev. D* **87** 105020; Muñoz-Castañeda J M and Mateos Guilarte J 2015 *Phys. Rev. D* **91** 025028.

[5] Díaz J I, Negro J, Nieto L M and Rosas-Ortiz O 1999 *J. Phys. A: Math. Gen.* **32** 8447; Gadella M, Heras F J H, Negro J and Nieto L M 2009 *J. Phys. A: Math. Theor.* **42** 465207; Gadella M, Negro J, Nieto L M 2009 *Phys. Lett. A* **373** 1310; Gadella M, Glasser M L and Nieto L M 2011 *Int. J. Theor. Phys.* **50** 2144; Álvarez-Sánchez J J, Gadella M and Nieto L M 2011 *Int. J. Theor. Phys.* **50** 2161; Gadella M, Glasser M L and Nieto L M 2011 *Int. J. Theor. Phys.* **50** 2191.

[6] Gadella M, Mateos-Guilarte J, Muñoz-Castañeda J M and Nieto L M 2016 *J. Phys. A: Math. Theor.* **49** 015204.

[7] Gadella M, Mateos-Guilarte J, Muñoz-Castañeda J M and Nieto L M, *Adding δ'-point interactions to the theeth of the Dirac δ-comb potential* (in progress).